THE PENNSYLVANIA STATE UNIVERSITY
SCHREYER HONORS COLLEGE

JOHN AND WILLIE LEONE FAMILY DEPARTMENT OF ENERGY AND MINERAL ENGINEERING

Comparing Stress-Permeability Models for Various Lithologies through Permeability Compliance, Pore Spacing, and Bulk Modulus

MOHAMMAD E. ALNOAIMI
Spring 2022

A thesis
submitted in partial fulfillment
of the requirements
for a baccalaureate degree
in Petroleum and Natural Gas Engineering and Economics
with honors in Petroleum and Natural Gas Engineering

Reviewed and approved* by the following:

Brandon Schwartz
Assistant Research Professor
Thesis Supervisor

Eugene Morgan
Associate Head for Undergraduate Education
Honors Adviser

* Electronic approvals are on file.

ABSTRACT

We compare leading models for permeability evolution as a function of changing effective stress for various lithologies. In particular, the permeability compliance model as given in the literature is analyzed and compared to the cubic law, where changing pore aperture is cast in terms of pore spacing, bulk modulus, and changing pore pressure. Using equivalence relationships, it is shown that empirically derived values of permeability compliance for various lithologies can be used to determine the average spacing between pores used in the cubic law and related to the material strength of the rock (Bulk modulus). We derive equations for different rock types to calculate the pore network for each rock. In addition, we use values from the literature for bulk modulus for each lithology to calculate the permeability compliance and find excellent agreement with values for permeability evolution with changing stress found in the literature.

The cubic law predicts permeability loss under the same conditions based on the density of pores (number and size per unit volume). If a rock has a denser pore network (small *s/b*) it will have more pores available to accommodate a given deformation, leading to smaller permeability loss. We find that the term $(\frac{s}{b} * \frac{1}{K})$ found in the cubic law is proportional to the permeability compliance, where s is the average spacing between pores, b is the average pore diameter, and K is the bulk modulus. Therefore, permeability compliance can be viewed as a description of a rock's ability to resist permeability loss due to the pore network's compression during pressure-driven deformation.

TABLE OF CONTENTS

LIST OF FIGURES

LIST OF TABLES

ACKNOWLEDGEMENTS

I would like to convey my heartfelt gratitude to Dr. Brandon Schwartz, my research supervisor, for allowing me to conduct this research and providing me with vital assistance during this process. His dynamism, vision, genuineness, and motivation have all left an indelible impression on me. He showed me how to present my findings in the most clear and concise manner possible. Working and studying under his direction was an honor and a privilege. I am appreciative for everything he has done for me and would like to express my gratitude for his friendship and good humor.

I would also like to give a special thanks to my thesis advisor Dr. Eugene Morgan for his continues guidance and advice that helped me in writing this thesis.

I am extremely grateful to my parents for their love, support, and sacrifices for educating and preparing me for my future.

Chapter 1

Introduction

Subsurface engineering covers a broad range of disciplines encompassing oil and gas development, carbon sequestration, hydrogen storage, nuclear waste disposal, and gas storage. As such, an understanding of geologic media's response to changes in stress becomes paramount in predicting and accounting for many energy and waste applications relevant to society. A rock's ability to conduct fluid allows for secure energy storage, water resource management from freshwater aquifers, and geologic waste management. Furthermore, an understanding of subsurface response to changing stresses mitigates surface hazards including the risk of induced seismicity, freshwater fouling, and well integrity. Here, I explore the relationship between permeability—a rock's ability to conduct fluid through its pore space—and evolving stresses.

A rock's ability to conduct fluid is sensitive to changing stress, typically induced by pore pressure depletion. This has led to the development of stress-dependent permeability models, which must be recast for different lithologies due to differences in pore size (large fractures vs small nanopores), mineral stiffness (clays vs carbonates), and the geometry of the pore space. Differences in these variables among lithologies leads to a range of permeability responses to changing effective stress. Permeability can be very stress dependent specifically in lithologies such as cemented sandstones and vuggy carbonates, where the relationship is driven by the different texture each formation has. Fluid storage and conductivity in a formation depends on how interconnected pores are, which leads to natural relationships between porosity and permeability. Pores of each rock vary in sizes and dimensions as each sediment has its own porosity and permeability. Both of the previously mentioned properties are affected by stress (McKee, 1998). Because of differences in lithology characteristics such as mineral stiffness, orientation, and geological development, the stress-permeability relationship will be different for each lithology (Liu & Chen, 2018).

1.1 Stress-based permeability models

Effective stress is a function of overburden stress and pore pressure, and is defined as

$$\sigma' = \sigma_{ob} - \alpha P_p \tag{1}$$

where α is the dimensionless Biot poroelastic coefficient (Wang, 2017). As we move in production (P_p decreases), the decrease in pore pressure will cause the effective stress to increase. This will cause a decrease in the formation's permeability due to compression (compressive strain) of the rock, which is concentrated in the pore space available for fluid flow. In the context of petroleum engineering, the main control on changing effective stress in the subsurface is pore pressure depletion, leading to the development of stress-permeability models in terms of changing pore pressure. One such model is the concept of permeability compliance, which casts permeability evolution as an exponential decay function with changing pore pressure. Permeability compliance can be defined as a measure of how sensitive a change in permeability is to a change in pore pressure at a constant confining pressure. This relationship can be shown in the following equation:

$$\gamma = \frac{1}{k}\left(\frac{\delta k}{\delta P_p}\right) \tag{2}$$

where γ is the permeability compliance, k is permeability, and P_p is pore pressure (Yilmaz et al., 1994). Variations in pore pressure within a fractured rock causes permeability to fluctuate. In the case of hydraulic fracturing, the increase in fracture aperture and density leads to increased permeability but also increased permeability compliance, as fractures are more compliant than rock matrix. When injecting fluids into a hydraulically fractured reservoir, pressure usually changes quickly. In contrast, when producing from a hydraulically fractured reservoir, the pressure profile changes slowly. Unconsolidated reservoir's permeabilities are particularly sensitive to pore pressure changes, suggesting a higher permeability compliance (Yilmaz et al., 1994).

Other models cast permeability evolution as a function of effective stress and elastic constants in the exponential-decay function (Daley, 2006). Low effective stress results in a high permeability due to pore dilation, but also results in high elastic compliance. However, having a high effective stress will result in a low fluid permeability and a low elastic compliance (Daley, 2006). Elasticity of a material's compliance is made up of two components which are the compliance of its solid grains and the compliance of its varying grain borders and fractures as well as other flaws (Yilmaz et al., 1994). This variation leads to an impact on elastic compliance and permeability as well as some other properties. When interested in comparing permeability models, equivalent medium theories are the most applied methods of comparing elastic constants and permeability tensors (Zheng, 2015).

Permeability models that are cast in terms of porosity also must include changing effective stress. Low-porosity rocks that are subjugated to high effective stress experience minor changes in porosity, while their permeability drops dramatically. Relationships such as stress–permeability, stress–porosity, and permeability–porosity correlations have been described using empirical relationships based on laboratory data such as exponential or power laws that were measured while conducting studies on them. These models are very useful for predicting permeability evolution, but at very high effective stress they can become inaccurate. The exponential model for stress-dependent permeability is as follows (Durucan & Edwards, 1986):

$$k = k_0 e^{-A\sigma} \tag{3}$$

where σ is the effective stress which is a function of overburden density, pore pressure, and depth, k_0 is the initial permeability (at the initial stress state), and A is a coefficient determined in experiments. The permeability compliance γ from Eq. (2) is the A in Eq. (3). Rocks with low permeability have complicated variations in permeability and porosity when an increase in stress occurs. The permeability and porosity of high-permeability rock tend to decrease with increasing effective stress. Hydraulic behavior of a rock with low permeability is challenging to explain physically due to the lack of precision in low-permeability measurements (Klinkenberg, 1941; Javadpour, 2009). The following empirical function was developed by Walsh (1981):

$$k = k_0 \left[LOG \left(\frac{\sigma_h}{\sigma} \right) \right]^3 \tag{4}$$

Which relates permeability to effective stress and the $\sigma_h$is the effective stress at initial permeability.

1.2 Geometric permeability models

Other permeability models explore permeability evolution not as a function of changing stress, but of how the change in stress changes other properties. The Katz-Thompson equation links the change in permeability to the change in pore compressibility (Katz et al, 1986).

$$k = \theta r^2 \phi^m \tag{5}$$

Where φ is porosity, r is the pore throat size that regulates permeability, m is a cementation factor, and θ represents a form factor. In each porous medium various correlations are used differently. For example, the Katz-Thompson equation is used differently than the Carmen-Kozeny equation (porosity-cubed divided by surface area-squared) where it does not yield a particular surface area to measure permeability (Kozeny, 1927; Carman, 1937; Adenutsi et al., 2019). The Carman–Kozeny correction is a formula used in fluid dynamics to compute the pressure decrease of a fluid moving through a densely packed solid substrate (Adenutsi et al., 2019). When the effective pore throat radius and the equation are both utilized, the analysis becomes much harder because the pore throat radius and porosity change with applied stress. It's much easier to understand the relationship between porosity and permeability under varying stress circumstances when a porosity-permeability connection like the first equation is employed.

Stress-permeability models depend on the sensitivity of the lithology to stress-induced compaction. Soft sandstones and fractured rocks are examples of stress sensitive rocks (Coyner, 1977). One reason for stress sensitivity is the shape of pores, often called the shape factor. The permeability of rocks with high shape factors (slit-like pores) which deform in a manner similar to that of fractured rocks may be described by a Walsh permeability relationship (Walsh, 1981):

$$k = k_o \left(1 - \sqrt{2}\frac{\epsilon}{a_0} ln\frac{P}{P_0}\right)^3 \quad (6)$$

where a_0 is the half-aperture of pores, which measures how much of the opposite side of a fracture are in touch at the reference permeability and pressure, k_0 and P_0 respectively. As previously stated, pressure decreases when production from a well occurs. This may result in a reduction in the reservoir's permeability which may lead to a reduction to the production flow rate. According to the suggested pore-shell model, this results in an effective stress coefficient larger than one. The experimental results of the permeability tests are thus congruent with the microstructural approach (Gao & Ghassemi, 2017). The state-space description is considered a feasible characterization of permeability development with major stresses. It is appropriate for geomechanics situations that have varying stress rates that are a result of operations such as deep excavations.

1.3 Influence of lithology on permeability evolution

The lithology of a sample determines the stress-permeability relationship, as well as the resulting fluid flow during pressure depletion. Coal has a complex permeability response, due to a dual-permeability system and internal swelling from adsorption (Harpalani & Schraufnagel, 1990).

Permeability enhancement due to depletion in coal mines leads to negative environmental impacts from methane emissions, which can be minimized by draining gas from original seams before it enters operating areas (Durucan & Edwards, 1986). By understanding the coal permeability's dependence on pore pressure, methane could be released from coal strata and transferred to facilities—the permeability of the formation makes this process feasible. However, coal also tends to have low permeability.

Zhou and Sachdeva (2010) deduced an effective stress relationship for limestone permeability using constant permeability measurements in a triaxial cell at various confining pressures and pore pressure conditions. Due to its stress-permeability relationship, the Cobourg limestone is considered as a suitable site for a deep geologic repository with excellent lateral stability, extremely low horizontal and vertical hydraulic conductivity, and multiple low permeability barriers (Baghbanan & Jing, 2008; Zhou & Sachdeva, 2010). Furthermore, Glowacki and Selvadurai (2016) have completed studies on the Indiana limestone, where groundwater flow is a factor that affects geo-environmental areas. Examples of that are geological disposal of hazardous and toxic compounds which rely on the rocks' permeability.

Sandstone has a wide range of stress-permeability responses, based on other mineral components present and if the sandstone is loosely consolidated or tight. In Adenutsi et al (2019), a CMS-300 permeameter was used to investigate the stress-permeability relationship of sandstone, carbonate and fractured cores. The relationship between porosity and permeability was analyzed using a Carmen-Kozeny correlation with a changing porosity exponent and rising stress. Different porosity exponents correlate with different rock formations. For example, the porosity exponent of tight sandstone is found to be two. Carbonate cores are much more responsive to applied stress, and they had greater porosity exponents. In some cases, it is possible for the porosity exponent to be relatively large in certain circumstances in cores that have high variability such as carbonates. These types of carbonates are used to differentiate between the porosity of conductive and non-conductive materials.

Relationships between permeability and stress are often described as characteristics of the porosity (pore geometry, pore density, connectedness) or material strength (bulk modulus, fracture stiffness). However, most models do not incorporate both considerations (Palmer, 2009). Here, we explore equivalencies between porosity/pore-geometry models for stress-dependent permeability and permeability compliance as defined in Yilmaz et al (1994) as a function of evolving stress. Next, we examine the derivation of the cubic law in terms of pore spacing and compare it to permeability compliance. We are able to isolate the term for pore spacing (inverse of pore density, i.e. void volume per unit rock volume) using permeability compliance. We explore the relationship between pore density and permeability compliance and find good agreement between these two models while presenting our own model in terms of pore geometry and mechanical properties.

Chapter 2

Methodology

To obtain our results, we will derive both the cubic law equation in terms of *s/b* and P_p/K and the permeability compliance equation. Then, we will find the equivalence relationships between the two equations and find *s/b* and γ. We use *s/b* as a proxy for pore density, or availability of pores to compress during increase in stress. As *s/b* increases, fewer pores are available to distribute compressive strain leading to permeability loss.

2.1 Cubic law

The cubic law is derived from first principles using the Navier-Stokes equations assuming two infinite acting parallel plates (Bai & Elsworth, 2000). The result is a definition of permeability in terms of fracture aperture and spacing between fractures:

$$k = \frac{b^3}{12\,s} \tag{7}$$

where b is the fracture or pore aperture and s is the average spacing between fractures or pores. Therefore, initial permeability can be defined as

$$k_o = \frac{b_0^3}{12\,s_o} \tag{8}$$

In this equation, spacing is not changing. Thus, we have two constants. If we have two permeabilities k and k_o we can divide the equations above to get

$$\frac{k}{k_o} = \frac{b^3}{12\,s} * \frac{12\,s_o}{b_0^3} \tag{9}$$

Because pores are soft compared to matrix, and because s >> b, s does not change during deformation, as strain is concentrated in the pore space (Bai & Elsworth, 2000). Therefore, spacing will cancel out yielding:

$$\frac{k}{k_o} = \frac{b^3}{b_o^3} \tag{10}$$

Which can be simplified to the cubic law below

$$\frac{k}{k_o} = \left(\frac{b}{b_o}\right)^3 \tag{11}$$

Dividing the new permeability with the original permeability represent the percent change in permeability. We can rearrange Eq. (11) as

$$\left(\frac{k}{k_o}\right)^{\frac{1}{3}} = \frac{b'}{b_o} \tag{12}$$

Where b' is the original aperture plus a positive or negative change. The right-hand side of Eq. (12) can also be cast as:

$$\left(\frac{k}{k_o}\right)^{\frac{1}{3}} = \frac{b_o + \Delta b}{b_o} \tag{13}$$

We can simplify our equation to

$$\left(\frac{k}{k_o}\right)^{\frac{1}{3}} = \frac{b_o}{b_o} + \frac{\Delta b}{b_o} \tag{14}$$

Or

$$\left(\frac{k}{k_o}\right)^{\frac{1}{3}} = 1 + \frac{\Delta b}{b_o} \tag{15}$$

This expression can be reintroduced into Eq. (11) to give

$$\frac{k}{k_o} = \left(1 + \frac{\Delta b}{b_o}\right)^3 \tag{16}$$

In this equation b_o is illustrated in the following picture:

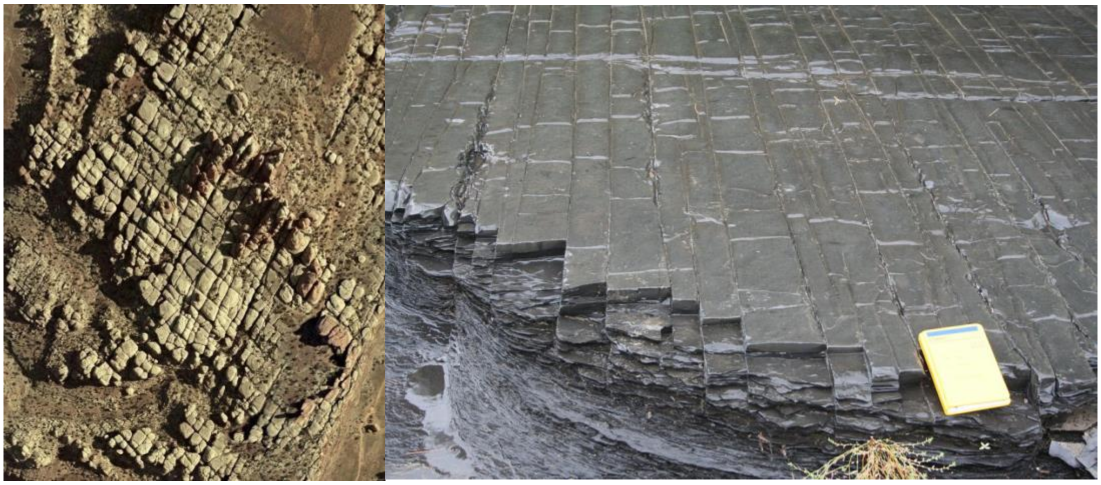

Figure 1 Set of joints

Fig. 1 shows a set of joints where spacing between fractures is visible and fractures create the conduits available for flow. We can apply this to flow channels that are much smaller than this, as

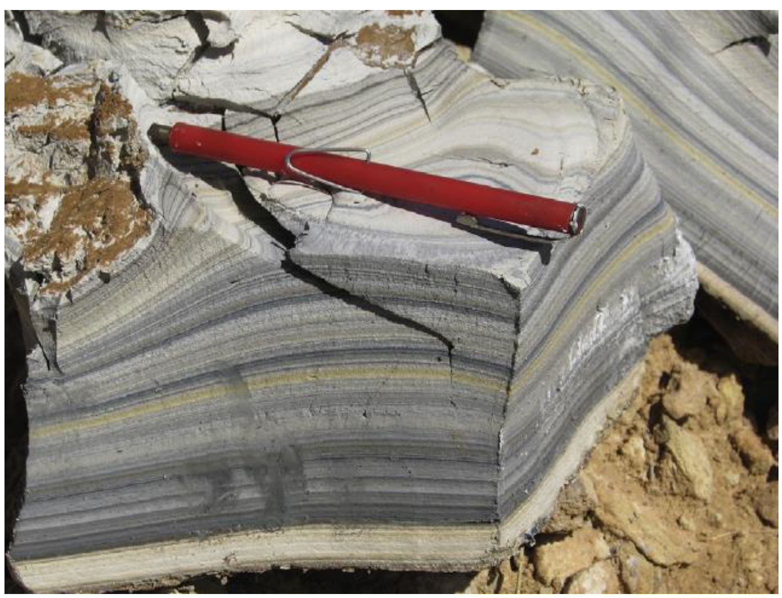

Figure 2 Parallel Bedding

shown in Fig. 2. Considering permeability parallel to bedding as illustrated in Fig. 2, flow occurs predominantly along bedding planes, or laminae, where porosity is concentrated. The structure between bedding planes consists of bridging asperities that create void space for flow. Therefore, we can use the same equation where in this case the b might be a few mm and s could be a meter between each. In this case the aperture is not millimeter but a micrometer. We will use this to calculate the change in permeability in a small rock. In this equation, we are mainly changing, Δb. If we have a system where we apply a force, we will have a stress. Since the mass of rock is not deforming, the grains are not getting smaller but moving into the pore space. Thus, we can define Δb as the strain ε multiplied by the spacing. If s >> b_0, then this relationship can be shown using the following equation (Bai & Elsworth, 2000):

$$\Delta b = s \cdot \varepsilon \tag{17}$$

If the volume shrank by 1%, especially if s is larger than b. The spacing change will change by the same 1%. This is useful because we have properties for strain. We can represent strain in 1 dimension using the following equation

$$\varepsilon = \frac{\Delta l}{l_o} \tag{18}$$

In the region of linear elastic behavior for rocks, we can relate strain to stress using Hooke's law below:

$$E = \frac{\sigma}{\varepsilon} \tag{19}$$

where σ is stress and ε is strain. Volumetric strain is defined as:

$$\varepsilon_v = \frac{\Delta\sigma}{K} \tag{20}$$

where K is bulk modulus. In rocks, we can use Eq. (20) to related changing stress with changes in pore pressure without changing the external stresses. Which means that any change in stress is due to pore pressure. Using this gives the following equation:

$$\varepsilon_v = \frac{\Delta p_p}{K} \tag{21}$$

A modulus tells us how much a rock deforms for a given change in pressure. In this sense, permeability compliance is a modulus, in that it shows what the change in permeability is for a given change in pressure. Here, we look at the change of strain for a change in pressure. We can plug this back in equation 17 which will give:

$$\Delta b = \varepsilon * s \tag{22}$$

or

$$\Delta b = \frac{\Delta P_p * s}{K} \tag{23}$$

Finally, we can replace Δb in Eq. (16):

$$\frac{k}{k_o} = \left(1 + \frac{\Delta P_p * s}{K * b_o}\right)^3 \tag{24}$$

2.2 Permeability compliance

Here, we have an equation of permeability that is measuring the change in pressure and converting it to change in permeability. This is also what permeability compliance is measuring too. According to Nguyen et al. (2020), permeability compliance is defined as:

$$\frac{k}{k_0} = e^{-\gamma P} \tag{25}$$

Or

$$k = k_0 e^{-\gamma P} \tag{26}$$

We can define permeability compliance γ as

$$\gamma = \frac{1}{k} * \frac{\Delta k}{\Delta p} \tag{27}$$

Or

$$\gamma = \frac{1}{\Delta p} * \frac{\Delta k}{k} \tag{28}$$

Or

$$\gamma = \frac{\frac{\Delta k}{k}}{\Delta p} \tag{29}$$

which agrees with Eq. (2). In some rocks, changing the pressure will yield a large γ and other rock will have a small γ.

2.3 Equivalence relationships

We will combine our two equations derived above to get:

$$\frac{k}{k_o} = \left(1 + \frac{\Delta p_p * s}{K * b_o}\right)^3 = e^{-\gamma \Delta P_p} \tag{30}$$

Or

$$\left(1 + \frac{\Delta p_p * s}{K * b_o}\right)^3 = e^{-\gamma \Delta P_p} \tag{31}$$

But since we are applying an external pressure and pore pressure is always decreasing. The equation can be written as:

$$\left(1 - \frac{\Delta p_p * s}{K * b_o}\right)^3 = e^{-\gamma \Delta P_p} \tag{32}$$

Here, we can see that permeability compliance is description of the rocks to resist deformation for a given change in pore pressure time its pore network configuration. We can re-arrange this equation in two different ways by solving for γ or $\frac{s}{b_o}$

To solve for γ:

$$ln\left(1 - \frac{\Delta p_p * s}{K * b_o}\right)^3 = -\gamma \Delta P_p \tag{33}$$

Algebra gives:

$$3ln\left(1-\frac{\Delta p_p * s}{K * b_o}\right) = -\gamma \Delta P_p \tag{34}$$

$$\gamma = -\frac{3}{\Delta P_p} ln\left(1-\frac{\Delta p_p * s}{K * b_o}\right) \tag{35}$$

In addition, to solve for $\frac{s}{b_o}$

$$\left(1-\frac{\Delta p_p * s}{K * b_o}\right)^3 = e^{-\gamma \Delta P_p} \tag{36}$$

Algebra gives:

$$1-\frac{\Delta p_p * s}{K * b_o} = e^{-\frac{1}{3}\gamma \Delta P_p} \tag{37}$$

$$\frac{\Delta p_p * s}{K * b_o} = -e^{-\frac{1}{3}\gamma \Delta P_p} + 1 \tag{38}$$

$$\frac{s}{b_o} = \frac{K}{p} - \frac{K}{p} e^{-\frac{1}{3}\gamma \Delta P_p} \tag{39}$$

Chapter 3

Results

Table. 1. Literature values for Bulk Modules (K) and Permeability Compliance (PC)

Rock Type	K (GPA)	k (psi)	Source	γ (psi^-1)	Source
Tight Sandstones	7	1.02E+06	Wang et al. (2017)	3.00E-04	Yale (1984)
Westerly granite	5	7.25E+05	James et al. (1976)	2.30E-04	Brace et al. (1968)
Carrara marble	50	7.25E+06	John et al. (1989)	3.20E-04	Fisher and Paterson (1992)
Basalt	25	3.63E+06	Adam et al. (2013)	7.00E-04	Nguyen et al. (2020)
Shale	10	1.45E+06	Schwartz et al. (2019)	4.00E-04	Yasser et al. (2011)
Indiana Limestone	22	3.19E+06	David et al. (1995)	1.38E-05	David et al. (1995)
Sandstones	9	1.31E+06	David et al. (1995)	3.00E-04	David et al. (1995)
Carbonate (Estaillade)	72	1.04E+07	Bakhoriju et al. (2010)	2.80E-05	Dautriat et al. (2011)

Using the derived equation, I was able to range pressure from 100 psia to 5000 psia and calculate *S/b* for each lithology. This is shown below in table. 2. It is shown that *s/b* decreases as we increase pressure

Table. 2. Calculated S/b as a function of pressure drawdown – Part 1

Rock Types	Tight Sandstones	Westerly granite	Carrara marble	Basalt
Pressure	$\frac{s}{b}$	$\frac{s}{b}$	$\frac{s}{b}$	$\frac{s}{b}$
100	1.01E+02	5.53E+01	7.69E+02	8.35E+02
500	9.89E+01	5.45E+01	7.53E+02	7.98E+02
1000	9.65E+01	5.35E+01	7.33E+02	7.54E+02
1500	9.42E+01	5.25E+01	7.14E+02	7.13E+02
2000	9.19E+01	5.15E+01	6.96E+02	6.76E+02
2500	8.98E+01	5.05E+01	6.78E+02	6.41E+02
3000	8.76E+01	4.96E+01	6.61E+02	6.08E+02
3500	8.56E+01	4.87E+01	6.45E+02	5.78E+02
4000	8.36E+01	4.78E+01	6.29E+02	5.50E+02
4500	8.17E+01	4.70E+01	6.14E+02	5.24E+02
5000	7.98E+01	4.61E+01	5.99E+02	4.99E+02

Table. 3. Calculated S/b as a function of pressure drawdown – Part 2

Rock Types	Shale	Indiana Limestone	Sandstones	Carbonate (Estaillade)
Pressure	$\frac{s}{b}$	$\frac{s}{b}$	$\frac{s}{b}$	$\frac{s}{b}$
100	1.92E+02	1.46E+01	1.30E+02	9.73E+01
500	1.87E+02	1.46E+01	1.27E+02	9.71E+01
1000	1.81E+02	1.46E+01	1.24E+02	9.69E+01
1500	1.75E+02	1.46E+01	1.21E+02	9.67E+01
2000	1.70E+02	1.46E+01	1.18E+02	9.65E+01
2500	1.64E+02	1.46E+01	1.15E+02	9.62E+01
3000	1.59E+02	1.46E+01	1.13E+02	9.60E+01
3500	1.54E+02	1.45E+01	1.10E+02	9.58E+01
4000	1.50E+02	1.45E+01	1.07E+02	9.56E+01
4500	1.45E+02	1.45E+01	1.05E+02	9.54E+01
5000	1.41E+02	1.45E+01	1.03E+02	9.51E+01

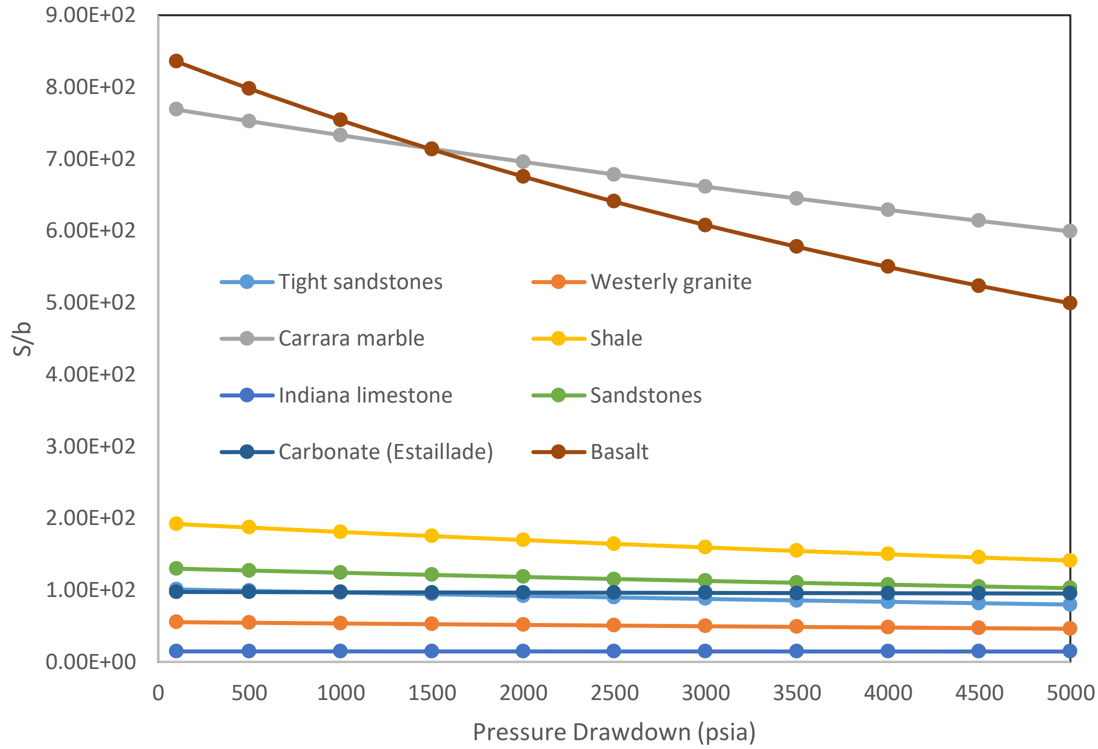

Figure 3 S/b as a function of Pressure Drawdown (psia)

Using the equation, we derived to calculate permeability compliance, I assumed different *s/b* values for each rock type based on the fact that *s/b* will decrease as we select a more porous sample. Figure 3 shows how different *s/b* will change as a function of pressure drawdown. Where most rocks did not face a huge change when compared to basalt and Carrara marble.

Table. 4. Calculated permeability compliance for different rock types

Rock type	$\frac{s}{b}$	γ(psia^{-1})
Tight Sandstones	101	3.00E-04
Westerly granite	55.5	2.30E-04
Carrara marble	769.43	3.20E-04
Basalt	836.26	7.00E-04
Shale	192	4.00E-04
Indiana Limestone	14.67	1.38E-05
Sandstones	129.88	3.00E-04
Carbonate (Estaillade)	97.42	2.80E-05

We can also calculate $\frac{k}{k_0}$ using both equations shown below:

Cubic law:

$$\left(1-\frac{\Delta p_p * s}{K * b_o}\right)^3 \quad (40)$$

And the PC law

$$e^{-\gamma \Delta P_p} \quad (41)$$

We compared our results for Westerly Granite to Yilmaz et al (1994) as shown in Table 4. In addition, we plotted the change in permeability as a function of pressure drawdown for each rock type.

Table. 5. Calculated $\frac{k}{k_0}$ for Westerly granite using cubic and PC law

Westerly Granite						
Derived equation			Yilmaz (1994)			
$\Delta \boldsymbol{p}$ (psia)	$\frac{k}{k_0}$ (Cubic Law)	$\frac{k}{k_0}$ (PC Law)	effective pressure (psia)	Δp (psia)	k (md)	$\frac{k}{k_0}$
0	1.000	1.000	53.7	0.0	724.7	1
100	0.977	0.977	89.5	35.8	792.8	0.99
200	0.955	0.955	116.3	62.6	781.9	0.99
300	0.933	0.933	170.0	116.3	716.4	0.98
400	0.911	0.912	196.8	143.1	697.3	0.96
500	0.890	0.891	241.6	187.9	727.2	1.00
600	0.868	0.871	474.2	420.5	601.6	0.83
700	0.848	0.851	483.1	429.4	566.2	0.78
800	0.827	0.832	518.9	465.2	612.4	0.84
900	0.807	0.813	876.7	823.1	478.5	0.66
1000	0.788	0.794	984.1	930.4	478.4	0.66
1500	0.694	0.708	993.0	939.4	538.3	0.74
2000	0.608	0.631	1073.6	1019.9	467.3	0.64
2500	0.529	0.562	1100.4	1046.7	494.6	0.68
3000	0.457	0.501	1601.4	1547.7	474.9	0.66
3500	0.392	0.446	1610.3	1556.7	428.5	0.59
4000	0.334	0.398	2102.4	2048.7	387.1	0.53
4500	0.282	0.354	4052.7	3999.0	204.9	0.282
5000	0.235	0.316	X	X	X	X

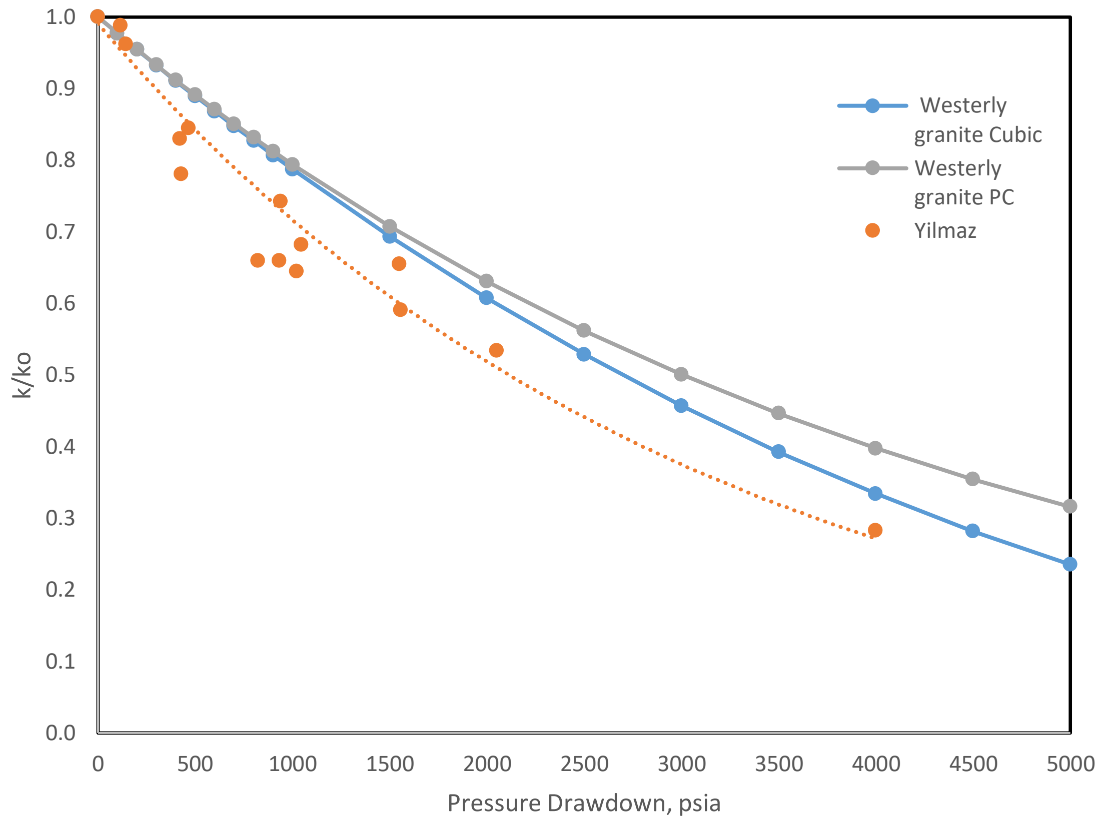

Figure 4 Permeability as a function of pressure drawdown (Westerly granite)

Figure 4. compares the results obtained from the Permeability compliance equation and the cubic law with (Yilmaz. 1994). We observed how the permeability will change as a function of pressure drawdown in psia. As seen in the plot, both results were close and showed that our rock sample will lose permeability with the change in pressure.

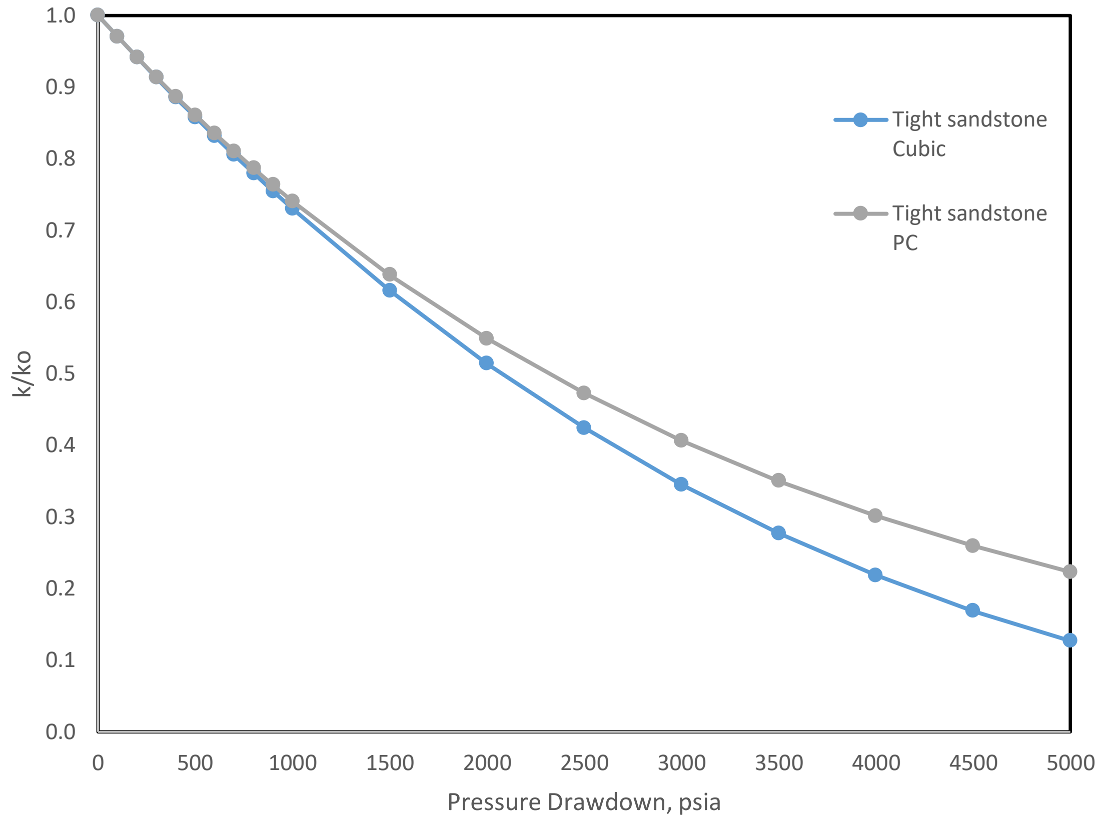

Figure 5 Permeability as a function of pressure drawdown (Tight sandstone)

Figure 5. compares the results obtained from the Permeability compliance equation and the cubic law. The plot shows how permeability change as a function of pressure drawdown in psia. As seen in the plot, it is found that our rock sample will lose permeability when we face a change in pressure.

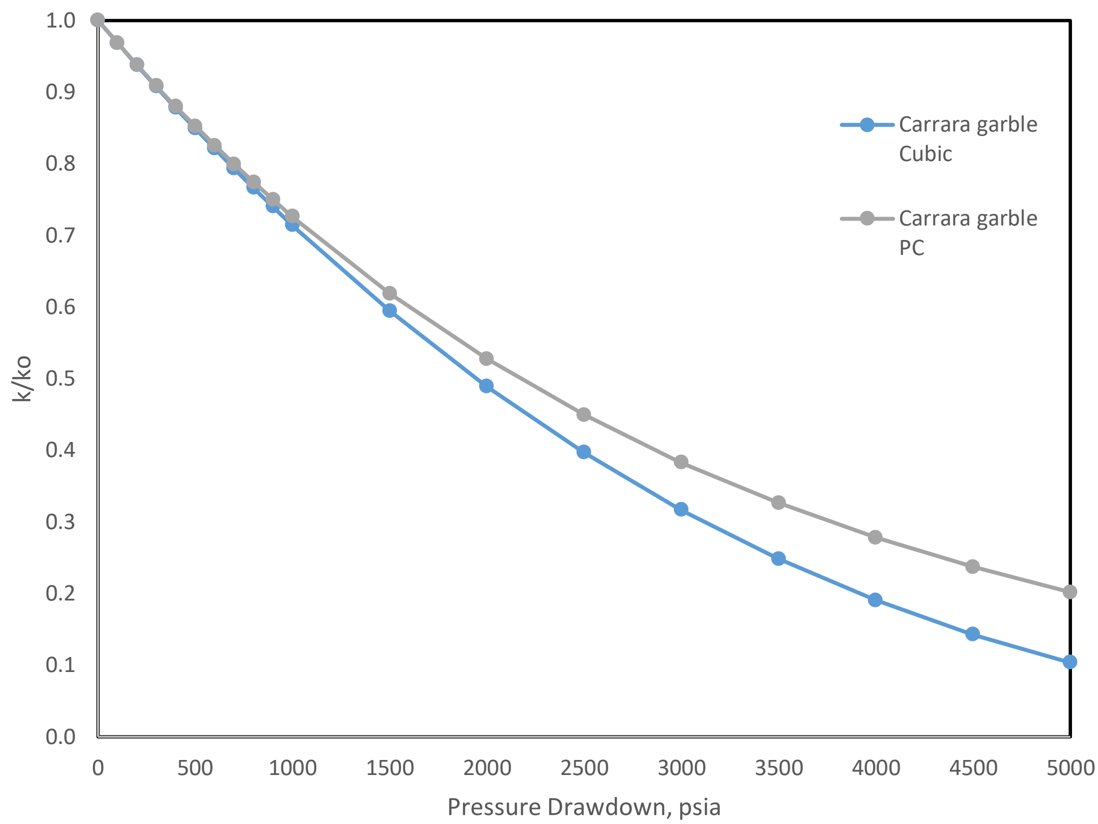

Figure 6 Permeability as a function of pressure drawdown (Carrara marble)

Figure 6. compares the results obtained from the Permeability compliance equation and the cubic law. The plot shows how permeability change as a function of pressure drawdown in psia. As seen in the plot, it is found that our rock sample will lose permeability when we face a change in pressure.

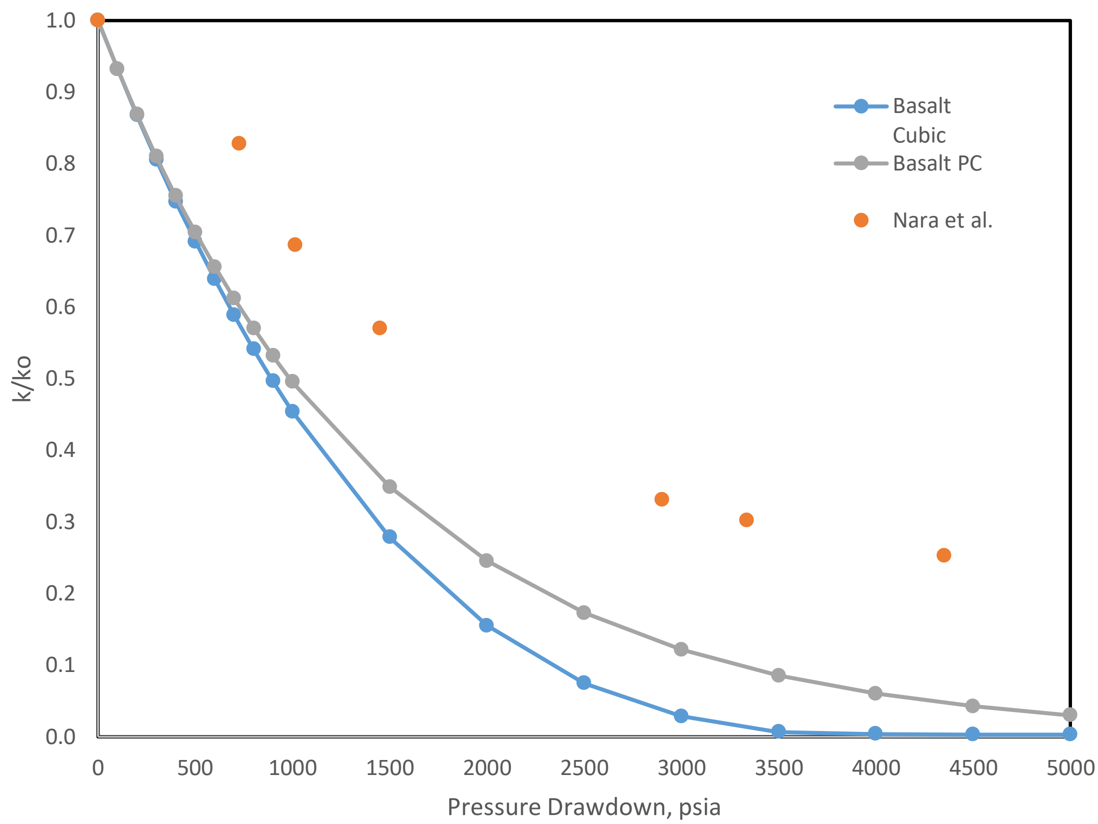

Figure 7 Permeability as a function of pressure drawdown (Basalt)

Figure 7. compares the results obtained from the Permeability compliance equation and the cubic law with (Nara et al., 2011). The plot shows how permeability change as a function of pressure drawdown in psia. As seen in the plot, both results were close and showed that the rock sample will lose permeability with the change in pressure.

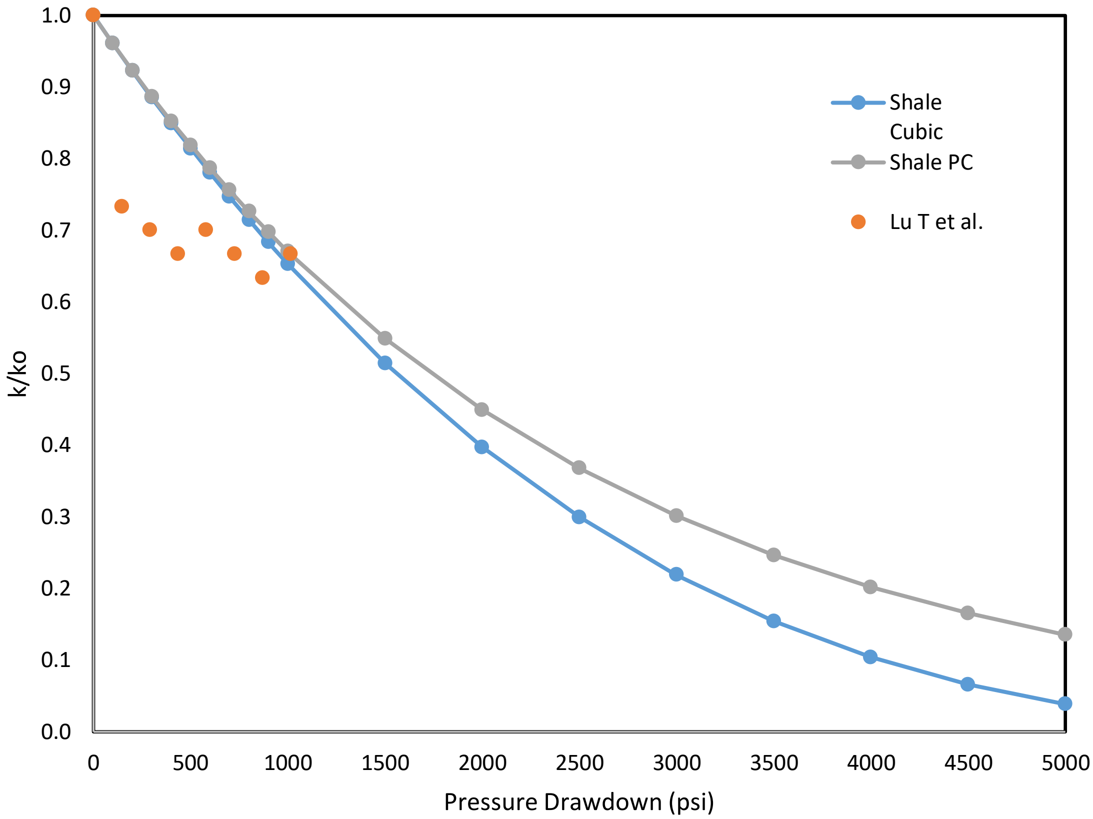

Figure 8 Permeability as a function of pressure drawdown (Shale)

Figure 8. compares the results obtained from the Permeability compliance equation and the cubic law with (Lu T et al., 2019). The plot shows how permeability change as a function of pressure drawdown in psia. As seen in the plot, both results were close and showed that the rock sample will lose permeability with the change in pressure.

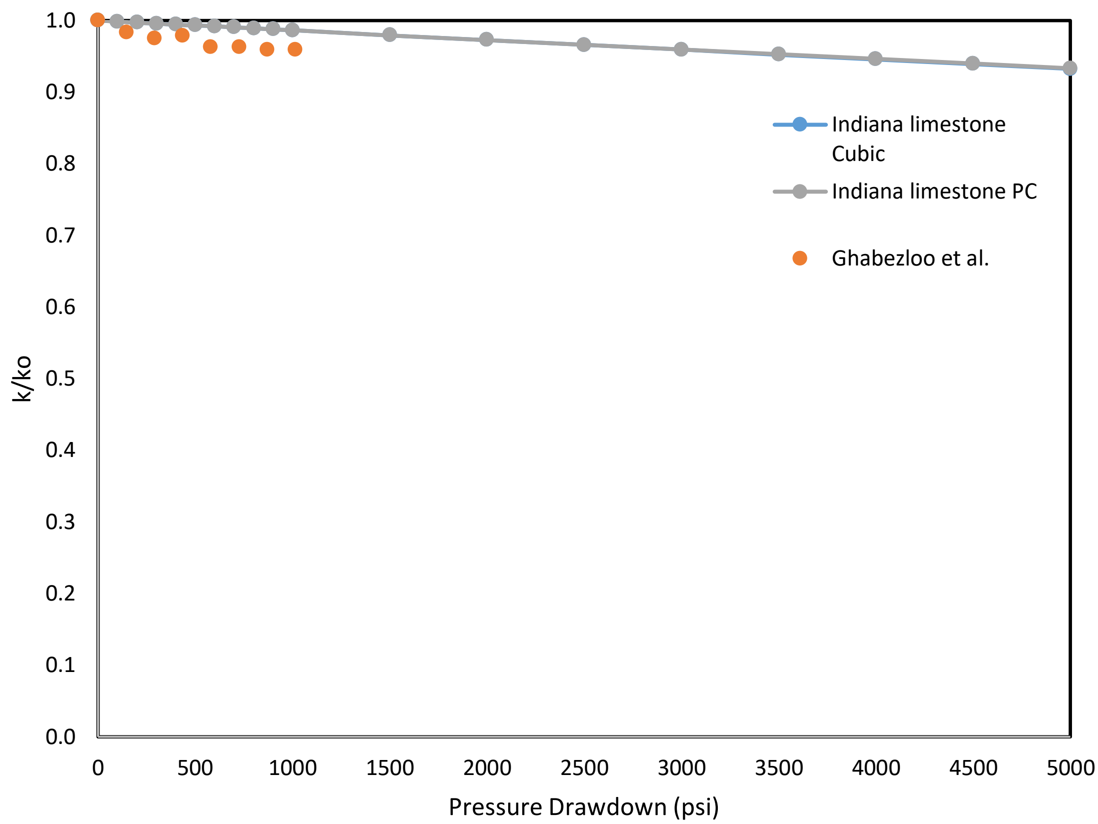

Figure 9 Permeability as a function of pressure drawdown (Indiana limestone)

Figure 9. compares the results obtained from the Permeability compliance equation and the cubic law with (Ghabezloo et al., 2009). The plot shows how permeability change as a function of pressure drawdown in psia. As seen in the plot, both results were close and showed that the rock sample will lose permeability with the change in pressure. But it is found that limestones do not lose much permeability and have smaller slopes when compared to other rock types.

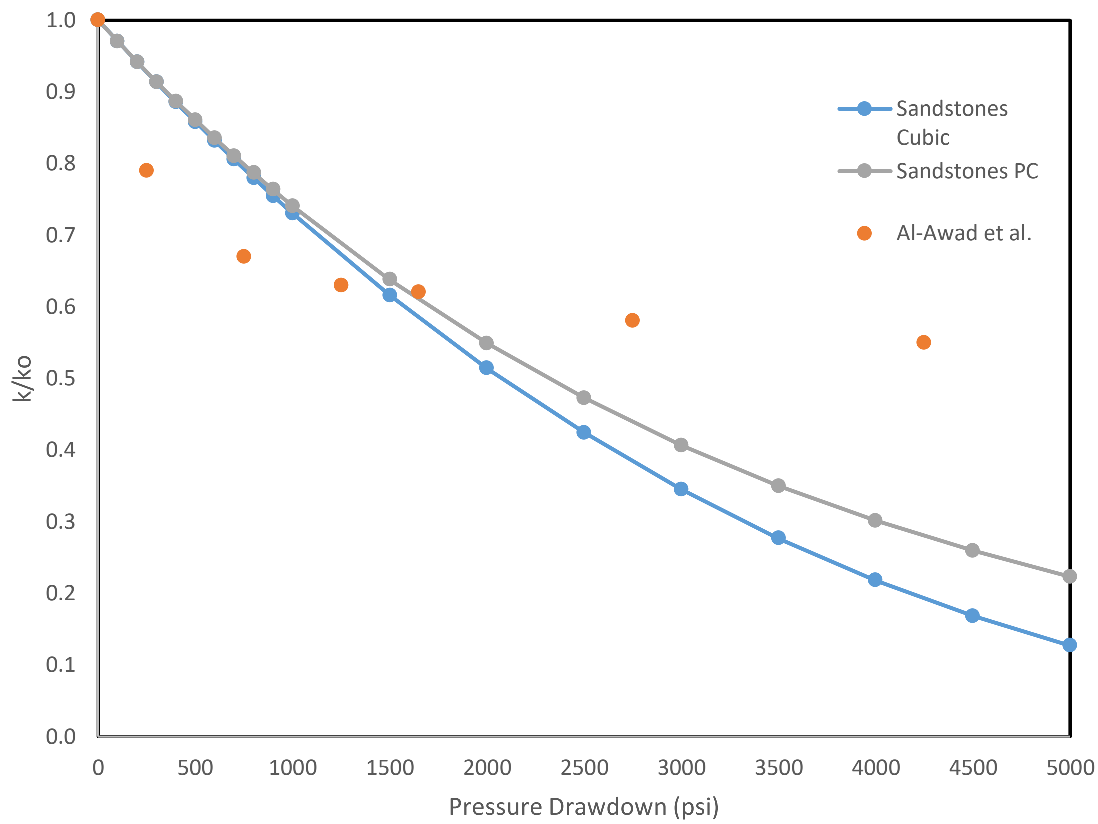

Figure 10 Permeability as a function of pressure drawdown (Sandstones)

Figure 10. compares the results obtained from the Permeability compliance equation and the cubic law with (Al-Awad, 2001). The plot shows how permeability change as a function of pressure drawdown in psia. As seen in the plot, both results were close and showed that the rock sample will lose permeability with the change in pressure.

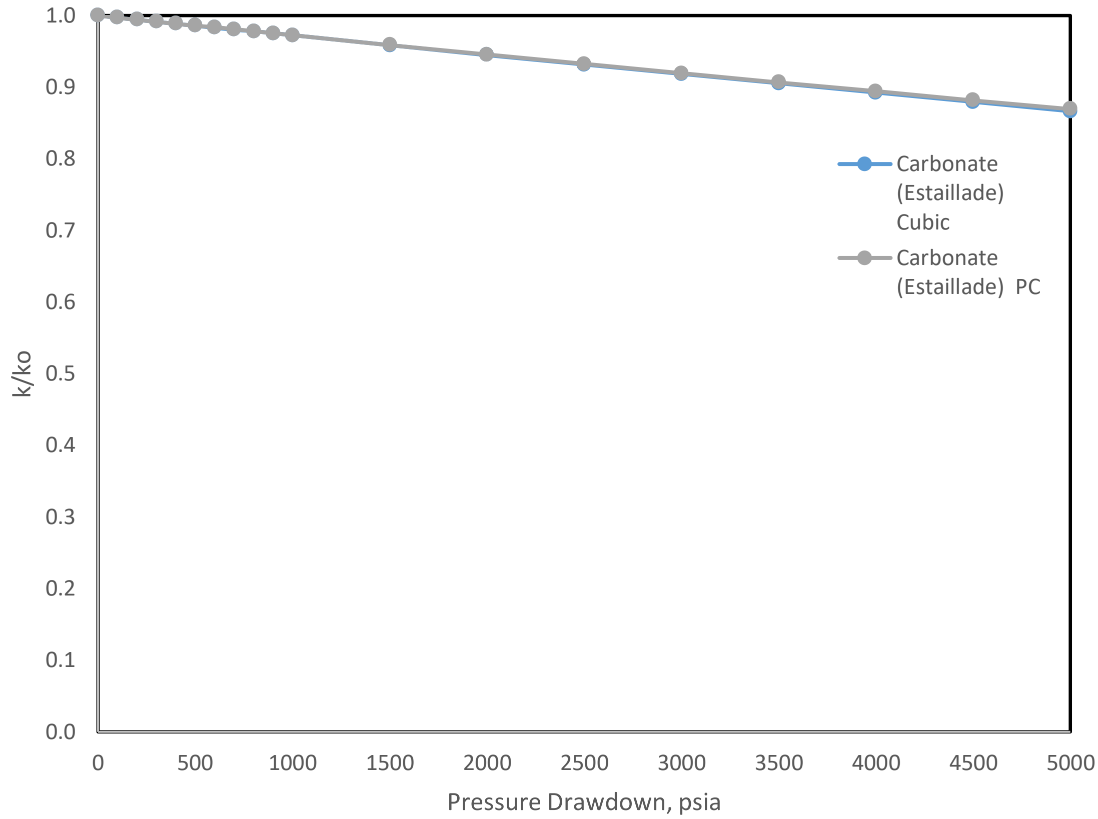

Figure 11 Permeability as a function of pressure drawdown (Carbonate)

Figure 11. compares the results obtained from the Permeability compliance equation and the cubic law. The plot shows how permeability change as a function of pressure drawdown in psia. As seen in the plot, it is found that our rock sample will lose permeability when we face a change in pressure. But it is found that Carbonates do not lose much permeability and have smaller slopes when compared to other rock types.

We can combine all of our lithologies in one plot in order to investage how different does permeability as a function of pressure drawdown.

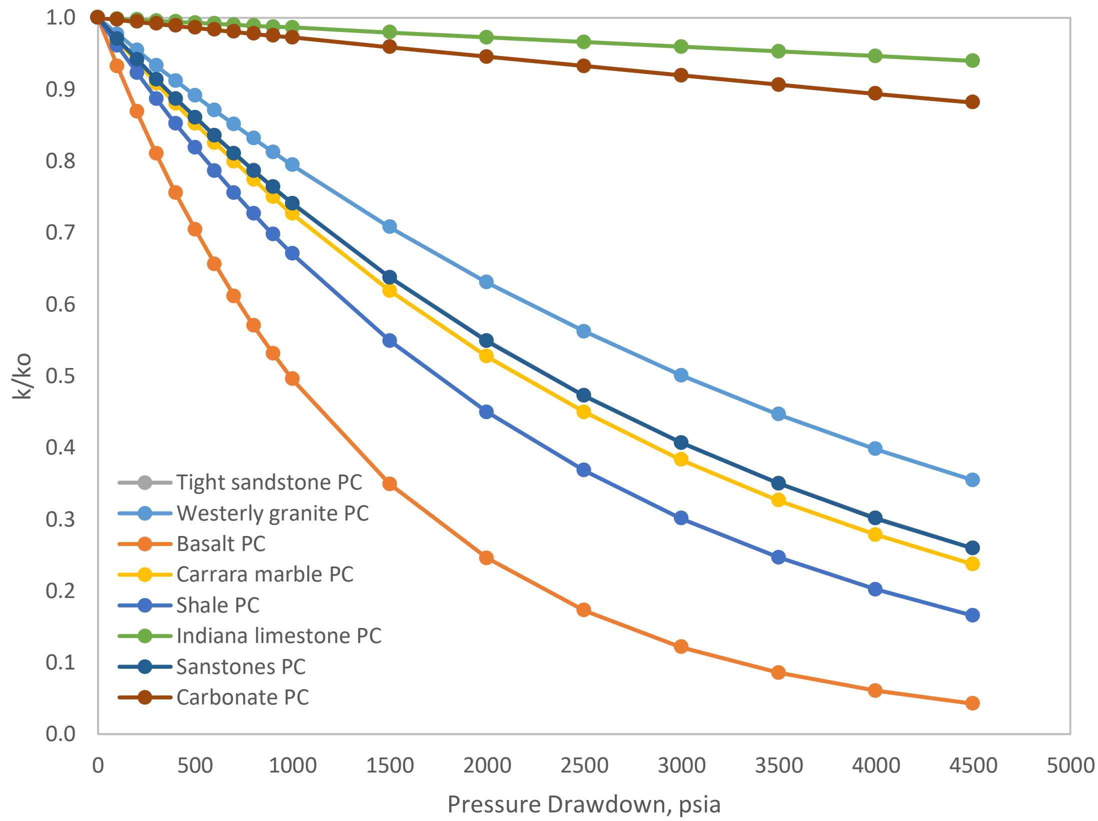

Figure 12 Permeability as a function of pressure drawdown

To validate our results, we re-created the figure from Nguyen et. al. (2020). Which investigate permeability change as a function of pressure drawdown for different values of Permeability compliance

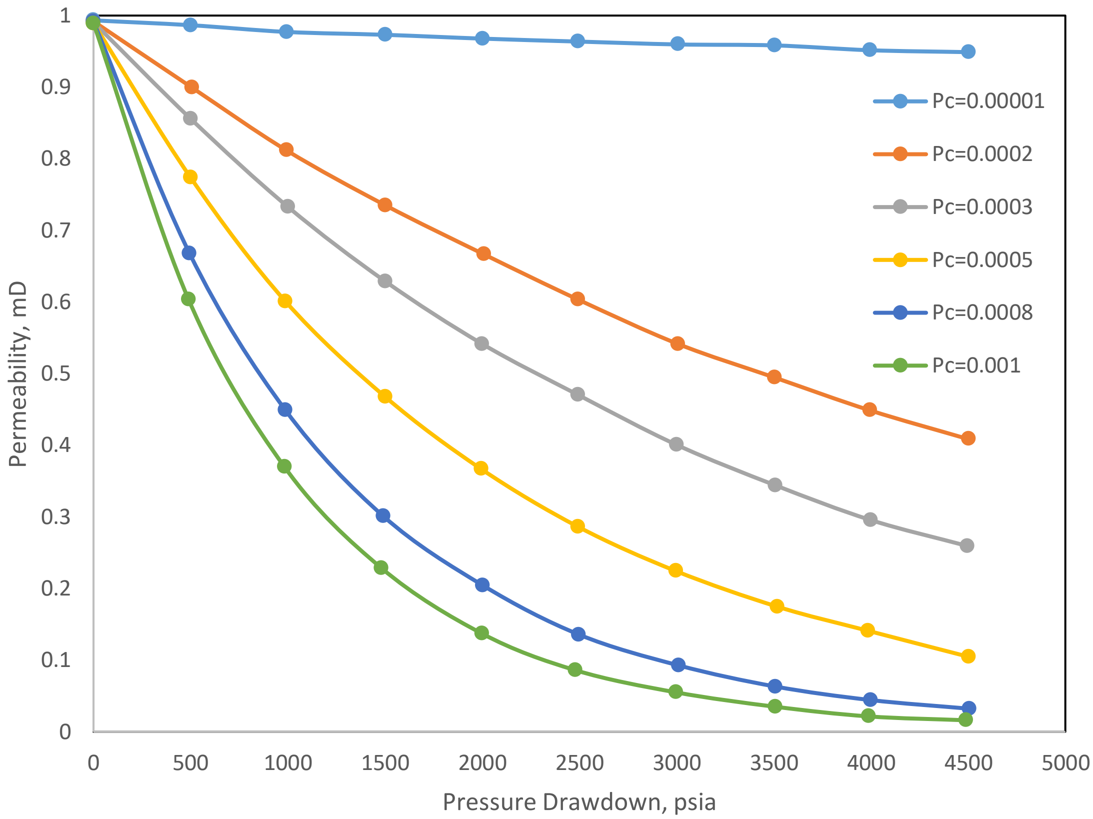

Figure 13 Re-created plot from Nguyen et al, (2020)

Figure 13. is a re-created plot found in Nguyen et al, (2020). It is found that samples with larger permeability compliance values tend to lose more permeability when pressure changes. On the other hand, sample with smaller permeability compliance loses less permeability. This is also shown in our results obtained from our two equations.

Chapter 4

Discussion

Permeability is an essential reservoir property. For many years, studies developed many functions to relate the permeability function with different variable like pressure change, stress change, formation dependent and fracture lengths and widths. Each function tends to be more accurate for different rock types. In some stress-dependent reservoirs, it has been found that the production of the reservoir can be dependent on the change in pressure and stress. To evaluate the overall production loss, some investigations were done on the permeability as well. (Raghavan and Chin, 2004) were able to develop numerical models to determine the impact of pressure drawdown and overburden stress on the permeability for two types of rocks. The following equation represents a linear relationship between the effective mean stress and permeability on a porous clastic rock,

$$k = k_o\left(1 - m\left(p_i - p_{wf}\right)\right) \tag{42}$$

Further studies were conducted by (Raghavan and Chin, 2004) on unconsolidated material. They found that the permeability changes as the rock porosity changes in the power-law relationship where n and the permeability at the reference porosity are determined experimentally. The relationship can be expressed as the following,

$$k = k_o\left(\frac{\phi}{\phi_o}\right)^n \tag{43}$$

(Yimaz, 1994) Started relating Permeability with initial permeability, permeability compliance, and difference between the initial pressure and flowing bottom hole pressure. He tried to introduce the permeability compliance and relate it to the permeability change with the pressure drawdown. Also, it was found that this relationship is close to the compressibility of the formation. Where an increase in compressibility will increase permeability compliance. The function that Yilmaz developed worked better for low porosity crystalline rocks.

$$k = k_o e^{-\gamma(p_i - pwf)} \quad (44)$$

(Nguyen, et al., 2013) Focused more on core lab analysis. They combined well test analysis and well logging to measure petrophysical properties of the reservoir. They found that the stress paths effects the reservoir properties like permeability. They focused more in weakly consolidated sandstones and found that there are a plastic deformation of the rock and permeability changes. They concluded that Permeability can be related to stress-strains for consolidated formations. This function can be expressed as:

$$k = k_0 e^{C\varepsilon_{eff}} \quad (45)$$

The evaluation of the productivity of a reservoir typically depends on three criteria: permeability, residual water saturation, and porosity. To compute the exact values for these variables at certain reservoir intervals, extensive coring needs to take place. Both porosity and water saturation values can be found using wireline logging, while permeability is obtained through DST or laboratory core analysis. However, the following empirical correlation was introduced by (Timur, 1969) to estimate the permeability of reservoir,

$$k = \frac{0.136 * \phi^{4.4}}{S_{wi}^2} \quad (46)$$

(Wyllie and Rose, 1950) worked on using electrical logs to find important reservoir parameters such as permeability. In addition, Tixier proposed a method to determine permeability from log data. He assumed that the exponent in the resistivity index-saturation relationship is 2. Also, he assumed that S_{wi} is related to permeability. The function concluded is as following:

$$k = \left(\frac{100 * \phi^{2.25}}{S_{wi}}\right)^2 \quad (47)$$

And

$$k = \left(\frac{100*\phi^2*(1-S_{wi})^{2.25}}{S_{wi}}\right)^2 \quad (48)$$

The permeability compliance function models the permeability relationship with pressure drawdown using an exponential decay function where the independent variable is stress. Different values for permeability compliance are basically from curve fitting. To be more specific, the larger γ is we will have a steeper slope. As we increase stress on the rock, it loses permeability faster. The permeability compliance relationship is useful but an empirical relationship. To find the correct value of γ. We need to fit an exponential equation to lab data. Which gives it an advantage because it can be used for any lithology.

On the other hand, the cubic law has more basis of physics because we can derive it from the Navier-Stokes equations. This equation incorporates pore density *(s/b)* and geomechanics *(P/K)* or just mechanical property of the rock. This makes it different from the permeability compliance function. The cubic law is developed for fracture flow, which gives it some limitation when used for small pores like shale. This is because pores usually do not behave identically to fractures. In addition, the Navier-Stokes law assumes Darcian flow, which might not work as much in nanopores where Darcy's law breaks down and Ficks law takes over. Since Darcy's law works with laminar flow, not diffusive flow. The Cubic law cannot model the behavior of a single fracture, it works best for fracture system where all the fractures are pointing in the same direction. To use the cubic law, we need to know if the joint sets are similar enough to pores in matrix rock where all these experiments are occurring. Darcy's law usually breaks down at 10 nm. Meaning that if we have pores that are 10 micrometers, we can safely assume that Darcy flow is still happening and therefore we can apply the cubic law.

Chapter 5

Conclusion

Permeability compliance is description of the rocks to resist deformation for a given change in pore pressure time its pore network configuration. Between two rocks that are too similar, if one rock has a smaller spacing. It will have more fracture available to accommodate a given deformation and thus we have less permeability loss.

The permeability compliance is related to the material strength of the rock (Bulk modules) and the pore network (S/b). It approximates the density of pore and explain how may pores and fracture exist for a given unit of rock. If S/b is large, this means that s is large when compared to b and there are very few fractures. On the other hand, if S/b is small, s is small is compared to b. This will be a highly porous system, and permeability does not change as much.

Using the literature, we were able to obtain values for permeability compliance and Bulk modulus. We used the equation derived before to calculate S/b for all different lithology. It was observed that S/b for all rock types tend to decrease as we increase the pressure. But, for most rock types, S/b decreased at a smaller rate. In which, it was almost constant through the pressure difference. On the other hand, Basalt and the Carrara marble faced a larger rate of decrease for S/b.

Using the derived equation for permeability compliance, we ranged S/b for different rock types from 10 to 1000 where 10 refers to porous rocks and 1000 refers to tight rocks. We compared the permeability compliance vales calculated with values from literature and found that they are close.

Furthermore, we were able to calculate k/k_0 for different lithologies using the cubic law and the permeability compliance law. It is found that the values initially are exact but as we keep increasing the pressure, we will see some deviation in which the Cubic law tend to be lower in the Permeability Compliance law. We also compared our calculations with literature to found that our results have the same trend. We also added all rock types into one graph. We found that Rocks with smaller Permeability compliance has a smaller change in permeability. While rocks with larger permeability compliance will face a higher decrease in permeability as the pressure increase. This relationship is also shown in the Nguyen et al. (2020) in which permeability decreased the less when PC = $1 * 10^{-5}\ psia^{-1}$ and decreased with the highest slope when PC = $1 * 10^{-3} psia^{-1}$

In addition, we can observe that the cubic law and the PC law match for all pressure when we are dealing with rocks that has smaller permeability compliance. For example, both Indiana limestone and Carbonate got an exact match when pressure decreased.

The general idea is that $(\frac{S}{b} * \frac{1}{K})$ has the same meaning as the permeability compliance, except in the first equation we are cubing the results while in the permeability compliance we are doing an exponential decay.

Appendix A

Nomenclature

k	Permeability
k_0	Initial Permeability
P	Pressure
p_b	Pore pressure
Δp	Pressure Difference
ϕ	Porosity
K	Bulk modules
γ	Permeability Compliance
$\frac{s}{b_0}$	Pore Network
b	Original Aperture
b'	Original Aperture plus a change
l_0	original length
Δl	change in length
σ	Stress
ε	Strain
s	Spacing

BIBLIOGRAPHY

Adenutsi, C. D., Li, Z., & Lai, F. (2019). Pore pressure variation at constant confining stress on water–oil and silica nanofluid–oil relative permeability. *Journal of Petroleum Exploration and Production Technology 9*, 2065–2079.

Al-Awad, M. N. (2001). Relationship Between reservoir productivity and pore pressure drop. Journal of King Saud University-Engineering Sciences, 13(1), 137-150.

Baghbanan, A., & Jing, L. (2008). Stress effects on permeability in a fractured rock mass with correlated fracture length and aperture. *International Journal of Rock Mechanics & Mining Sciences 45* , 1320–1334.

Bai, M., & Elsworth, D. (2000, April). Coupled processes in subsurface deformation, flow, and transport. American Society of Civil Engineers.

Brace, W. F. (1978). A Note on Permeability Changes in Geologic Material Due to Stress. *Pageoph, Vol. 116*, 628-632.

Carman, P. C. (1937). Fluid flow through granular beds. *Trans. Inst. Chem. Eng*., 15, 150-166.

Coyner, K. B. (1977). Effects of stress, pore pressure, and pore fluids on bulk strain, velocity and permiability in rocks. *Massachusetts intitute of technology*, 1-367.

Daley, T. M. (2006). Fractured reservoirs: An analysis of coupled elastodynamic and permeability changes from pore-pressure variation. *GEOPHYSICS 71*, 33-42.

Dong, J.-J. (2010). Stress-dependence of the permeability and porosity of sandstone and shale from TCDP Hole-A. *International Journal of Rock Mechanics and Mining Sciences*, 1141-1157.

Durucan, S., & Edwards, J. (1986). The effects of stress and fracturing on permeability of coal. *Mining Science and Technology, 3* , 205-216.

Gao, Q., & Ghassemi, A. (2017). Pore Pressure and Stress Distributions Around a Hydraulic Fracture in Heterogeneous Rock. *Rock Mech Rock Eng* , 3157–3173.

Ghabezloo, S., Sulem, J., Guédon, S., & Martineau, F. (2009). Effective stress law for the permeability of a limestone. International Journal of Rock Mechanics and Mining Sciences, 46(2), 297-306.

Głowacki, A., & Selvadurai, A. (2016). Stress-induced permeability changes in Indiana limestone. *Engineering Geology*, 122-130.

Harpalani, S., Schraufnagel, R. A. 1990. *Influence of Matrix Shrinkage and Compressibility on Gas Production From Coalbed Methane Reservoirs'*. In SPE Annual Technical Conference and Exhibition. Society of Petroleum Engineers.

Hua, Z., Klavera, J., J. S., Dewanckelec, J., & Amann-Hildenbranda, A. (2020). Stress sensitivity of porosity and permeability of Cobourg limestone. *Engineering Geology*, 105-108.

Huo, D., & Benson, S. M. (2016). Experimental Investigation of Stress-Dependency of Relative Permeability in Rock Fractures. *Transp Porous Med 113*, 567–590.

Javadpour, F. (2009). Nanopores and apparent permeability of gas flow in mudrocks (shales and siltstone). *Journal of Canadian Petroleum Technology*, *48*(08), 16-21.

Katz, A. J., & Thompson, A. H. (1986). Quantitative prediction of permeability in porous rock. *Physical review B*, *34*(11), 8179.

Klinkenberg, L. J. (1941, January). The permeability of porous media to liquids and gases. In Drilling and production practice. OnePetro.

Kozeny, J. (1927). Uber kapillare leitung der wasser in boden. *Royal Academy of Science, Vienna, Proc. Class I*, 136, 271-306.

Liu, H. H., & Chen, H. (2018). On the relationship between effective permeability and stress for unconventional rocks: Analytical estimates from laboratory measurements. *Journal of Natural Gas Science and Engineering*, 408-413.

Lu T, Xu R, Zhou B, Wang Y, Zhang F, Jiang P. Improved Method for Measuring the Permeability of Nanoporous Material and Its Application to Shale Matrix with Ultra-Low Permeability. *Materials*. 2019; 12(9):1567.

McKee, C. (1988). Stress-Dependent Permeability and Porosity of Coal and Other Geologic Formations. *SPE Formation Evaluation*, 81-91.

Nara, Y., Meredith, P. G., Yoneda, T., & Kaneko, K. (2011). Influence of macro-fractures and micro-fractures on permeability and elastic wave velocities in basalt at elevated pressure. Tectonophysics, 503(1-2), 52-5

Palmer, I. (2009). Permeability changes in coal: analytical modeling. International Journal of Coal Geology, 77(1-2), 119-126.

Schwartz, B., Huffman, K., Thornton, D., & Elsworth, D. (2019). A strain based approach to calculate disparities in pore structure between shale basins during permeability evolution. *Journal of Natural Gas Science and Engineering, 68*, 102893.

Shokouhi, P. (n.d.). Imaging elastodynamic and hydraulic properties of in-situ fractured rock: An experimental investigation exploring effects of dynamic stressing and shearing. *JGR: Solid Earth*.

T.C.Nguyena, S. D.-S. (2020). Pressure dependent permeability: Unconventional approach on well performance. *Journal of Petroleum Science and Engineering*, 107-358.

V, P., Tutuncu.A.N, Prasad.M, Kazemi.H, & Yin.X. (2011). An Experimental Study For Investigating the Stress Dependence of Permeability In Sandstones And Carbonates. *American Rock Mechanics Association*, 11-27.

Walsh, J. B. (1981). Effect of Pore Pressure and Confining Pressure on Fracture Permeability. *Int. J. Rock Mech. Min. Sci. & Geomech. Abstr. Vol. 18*, 429 to 435.

Wang, H. F. (2017). *Theory of linear poroelasticity with applications to geomechanics and hydrogeology*. Princeton University Press.

Yilmaz, O., Richard.C, Nolen-Hoeksema, & Nur, A. (1994). Pore pressure profiles in fractured and compliant rocks. *Geophysical Prospecting 42*, 693-714.

Zheng, J. (2015). Relationships between permeability, porosity and effective stress for low-permeability sedimentary rock. *International Journal of Rock Mechanics and Mining Sciences 78*, 304-318.

Zhou, D., & Sachdeva, R. (2010). Simple model of electric submersible pump in gassy well. *Journal of petroleum science and engineering*, 204-213#.

ACADEMIC VITA

MOHAMMAD ESSA ALNOAIMI

| alnoaimi7@gmail.com

EDUCATION

Schreyer's Honors College at the Pennsylvania State University, University Park, PA

- **Majors**: Petroleum and Natural Gas Engineering, B.S; Economics, B.S. May 2022
- **Honors**: Department of Energy and Mineral Engineering Student Marshal; Schreyer's Honors College; Royal Embassy of the Kingdom of Saudi Arabia Outstanding Student Award; College of EMS Merit Award; Bob Watson Scholarship in Petroleum and Natural Gas Engineering; Quentin and Louise Wood Honor Program 2020-2021 and 2021-2022; President's Freshman award
- **Relevant Coursework**: Money and Banking, Economics of Auctions and Procurements, Advanced International Trade, Advanced Econometrics, Applied Reservoir Engineering, Reservoir Modeling, Applied Reservoir Analysis and Secondary Recovery.

LEADERSHIP EXPERIENCE

Aramco Student Association, State College, Pennsylvania January 2020 – May 2021

President, Co-founder

- Co-Founded first Saudi Aramco Student Association in the United States, onboarding 193 members from 10 different majors
- Managed $12,500 in finances to organize general body meetings, field trips, and conference travels
- Engaged Aramco Scholars by organizing intramural sport tournaments between students

Penn State CrossFit Club, State College, Pennsylvania August 2020 - May 2021

THON Volunteer

- Fundraised $1500 to support kids fighting childhood cancer by organizing 3 sport competitions

Schreyer's Honors College, State College, Pennsylvania August 2020 - May 2022

Student Researcher

- Completed 14 Honors Credits including 3 honors classes and 11 credits of independent studies
- Worked with Prof. Brandon Schwartz to defend a thesis about deformation-induced changes to rock permeability correlated to changing dynamic bulk modulus

Society of Petroleum Engineers Student Chapter, State College, Pennsylvania August 2021 – May 2022

President

- First international student to be president of this Chapter
- Invited 16 professionals including SPE international leaders to host workshops
- Helped 146 students connect with major oil companies for internships and full-time jobs
- Motivated international students to be more active by inviting international industry leaders to host workshops and by hosting international culture nights

College of Earth and Mineral Science, State College, Pennsylvania August 2021 – May 2022

Student Ambassador

- Connect with undergraduate students currently enrolled at Penn State's 20 Commonwealth campuses considering College of EME Majors

ADDITIONAL INFORMATION

- **Proficient with:** MATLAB, Stata, Python, and Excel
- **Languages: Arabic and English**
- **Hobbies/Fun activities:** CrossFit, Golf, and Stargazing